한국음향학회지 제32권 제2호 pp. 95~103 (2013)
The Journal of the Acoustical Society of Korea Vol.32, No.2 (2013)
http://dx.doi.org/10.7776/ASK.2013.32.2.095

pISSN : 1225-4428
eISSN : 2287-3775

Performance Evaluation of Underwater Acoustic Communication in Frequency Selective Shallow Water

주파수 선택적인 천해해역에서 수중음향통신 성능해석

Kyu-Chil Park, Jihyun Park, Seung Wook Lee*, Jin Woo Jung*, Jungchae Shin*, and Jong Rak Yoon†

(박규칠, 박지현, 이승욱*, 정진우*, 신정채*, 윤종락†)

Department of Information and Communication Engineering, Pukyong National University
*Research and Development Department2, Gumi Plant Hanwha Co.

(Received January 8, 2013; accepted February 15, 2013)

ABSTRACT: An underwater acoustic (UWA) communication in shallow water is strongly affected by the water surface and the seabed acoustical properties. Every reflected signal to receiver experiences a time-variant scattering in sea surface roughness and a grazing-angle-dependent reflection loss in bottom. Consequently, the performance of UWA communication systems is degraded, and high-speed digital communication is disrupted. If there is a dominant signal path such as a direct path, the received signal is modeled statistically as Rice fading but if not, it is modeled as Rayleigh fading. However, it has been known to be very difficult to reproduce the statistical estimation by real experimental evaluation in the sea. To give an insight for this scattering and grazing-angle-dependent bottom reflection loss effect in UWA communication, authors conduct experiments to quantify these effects. The image is transmitted using binary frequency shift keying (BFSK) modulation. The quality of the received image is shown to be affected by water surface scattering and grazing-angle-dependent bottom reflection loss. The analysis is based on the transmitter to receiver range and the receiver depth dependent image quality and bit error rate (BER). The results show that the received image quality is highly dependent on the transmitter-receiver range and receiver depth which characterizes the channel coherence bandwidth.

Key words: Underwater acoustic communication, Underwater acoustic channel, Underwater image transmission
PACS numbers: 43.30.Cq, 43.30.Re, 43.30.ZK, 43.60.Dh

초 록: 천해에서 수중음향통신은 해면과 해저의 음향특성에 강한 영향을 받는다. 시변적인 해면 산란과 입사각에 좌우되는 해저손실에 의해 수중통신 시스템의 성능은 영향을 받게 되어 고속의 디지털 통신 성능은 저하된다. 우세한 직접파가 존재하면 통신채널은 Rice 페이딩, 그렇지 않은 경우 Rayleigh 페이딩으로 모델링된다. 그러나 실해역의 실험으로 이러한 통계적인 채널 모델링을 검증하는 것은 어려운 연구주제로 알려져 있다. 해면산란과 해저반사 손실이 수중음향통신에 미치는 영향의 근원적인 이해를 돕기 위하여 저자들은 이들의 영향을 정량화하기 위한 천해 해역에서 실험을 수행하였다. 이진 주파수 천이 변조 방식으로 영상을 전송하여 해면산란과 해저 입사각에 좌우되는 해저반사 영향을 송신기와 수신기간의 거리, 수신기 깊이에 따른 영상의 양호성과 비트 오류율로 평가하였다. 결론적으로 영상의 전송 성능은 채널의 일관성 대역폭을 결정하는 송수신기간의 거리 및 수신기의 깊이에 좌우된다.

핵심용어: 수중음향통신, 수중음향채널, 수중영상전송, 수중음향채널대역폭, 천해음향채널, 다중경로음향채널

I. Introduction

UWA communication system is highly sensitive to channel characteristic which depends on environmental parameters such as background noise, sea surface state, and depth dependent sound speed profile.[1-4] Special emphasis on the BER has been given to the effect of time-varying signal fluctuation due to sea surface roughness, which results in severe degradation of system

†**Corresponding author:** Jong Rak Yoon (jryoon@pknu.ac.kr)
Dept. of Information and Comm. Engr., Pukyong National University, Daeyeon 3dong, Namgu, Busan 608-737, Republic of Korea
(Tel: 82-2-629-6233; Fax: 82-2-629-6210)

performance by causing time and frequency spread of the transmitted signal. This is the fact that multipath time spread between the first and the last arrival path may span very much long comparing to bit interval and leads to severe Inter-Symbol Interference (ISI). In addition, all the paths but the paths propagating through the medium experience boundary reflection effects such as scattering at the sea surface and energy loss at sea bottom.

Special emphasis on the BER has been given to the statistics of time-varying signal fluctuation due to acoustical variation of the sea, which gives severe degradation of the communication system performance by causing time and frequency spread of the transmitted signal.[5-8] A frequency shift and an average reflection coefficient of a signal scattered by sea surface is given as a function of frequency and subtended angle.[9]

In previous study,[7,10] time-variant sea surface scattering is shown to be Rayleigh fading model and if there is a dominant direct path signal, then the equivalent low-pass received signal is modeled as Rice fading. However, it has been known to be very difficult to reproduce the statistical estimation by real experimental evaluation. In our previous experiment of 9 m depth river, BER and the received image quality were strongly dependent on the bottom path grazing angle and found to match well the channel coherence bandwidth of the multipath structure.[11] In general, a vertical and a horizontal channels are classified by a relative contribution of boundary reflected path intensity. The boundary reflected path of the former in which a transmitter and a receiver are located vertically, experiences high loss due to high grazing angle in boundaries but the boundary reflected path of the latter in which a transmitter and a receiver are located horizontally, experiences relatively low loss due to low grazing angle in boundaries. However it is not conclusive how each path contribute to channel coherence bandwidth considering transmitter- receiver range and receiver depth variations for a given transmitter position.[11]

In this study, image transmission performance of BFSK in 26 m depth of very shallow littoral is examined to figure out how the sea surface and the bottom boundaries affect the UWA channel and these are related to channel model. It is anticipated that transmitter-receiver range dependent acoustic channel performance is more clearly verified.

II. Channel Coherence Bandwidth in UWA Communication

In the time invariant discrete multipath channel, the channel's impulse response $h(\tau)$ for carrier frequency f_c is given as[8]

$$h_c(\tau) = \sum_{n=0}^{N} \alpha_n e^{-j2\pi f_c \tau_n} \delta(\tau - \tau_n) . \quad (1)$$

The α_n is the nth multipath signal's amplitude which depends on boundary reflection loss, path loss, and absorption loss, and τ_n is the nth multipath's delay time. In the time variant discrete multipath channel, the channel's impulse response $h(\tau;t)$ is given as[8,12]

$$h_c(\tau;t) = \sum_{n=0}^{N} \alpha_n(t) e^{-j2\pi f_c \tau_n(t)} \delta(\tau - \tau_n(t)) . \quad (2)$$

The autocorrelation function of $h(\tau;t)$ is defined as

$$R_h(\tau_1, \tau_2 ; \Delta t) = \frac{1}{2} E[h^*(\tau_1;t) h(\tau_2;t+\Delta t)]. \quad (3)$$

where Δt is an observation time difference between two different time instant $h(\tau;t)$. If the observation time difference Δt is set to be 0, then $R_h(\tau_1, \tau_2;0)$ becomes a Multipath Intensity Profile (MIP). Using the MIP, a channel coherence bandwidth B_c is evaluated.

A Root Mean Square (RMS) delay spread τ_{rms} is first calculated as

$$\tau_{rms} = \sqrt{\bar{\tau^2} - (\bar{\tau})^2} . \quad (4)$$

The average delay $\overline{\tau^2}$ and $\bar{\tau}$ are given as

$$\overline{\tau^2} = \frac{\sum_k P(\tau_k)\tau_k^{\,2}}{\sum_k P(\tau_k)}, \quad \bar{\tau} = \frac{\sum_k P(\tau_k)\tau_k}{\sum_k P(\tau_k)}. \tag{5}$$

where, $P(\tau_k)$ is an intensity of a *k*th path. The relationship between the effective delay spread τ_{rms}, and the B_c, is given as

$$B_c \approx \frac{1}{5\tau_{rms}}. \tag{6}$$

For a given digital signal transmission rate. The multipath frequency selectivity is evaluated by comparing the signal bandwidth B_s to channel coherence bandwidth B_c. If B_c is greater than the signal bandwidth B_s, the channel is defined as a frequency non selective channel which gives an error-free, stable signal transmission under no channel noise condition.

III. Experimental Procedure

Figure 1 shows a schematic layout of the experimental geometry for grazing-angle dependent boundary reflection effects on UWA communication. The experiment was conducted in 18 and 28 October 2011 in the bay of the Gwangan beach, which is located in east side of Busan city, Korea.

The effective surface wave height is about 0.7 m. Bottom sediment is sandy mud in experimental site. The tidal current flow is about 0.5 m/s. The bottom is sandy mud with a density and velocity of sound of 1567 kg/m^3, and 1540 m/s, respectively. CTD (instrument for continuous conductivity, temperature, and depth of ocean waters) is casted to measure water column properties during experiment. Two vessels of transmitter and receiver side are tethered to fix the transmitter-receiver range (Tx-Rx range). Therefore Doppler spread is ignored in data analysis. The range between the transmitter (ITC 1001) and receiver (B&K 8106) is set to be 50, 100 and 200 m and the depth of receiver is set as 5 and 20 m at each range. Transmitter depth is set as 7 m.

A noncoherent BFSK modem of 20 and 22 kHz carrier frequencies, is implemented for image transmission because of its robustness and implementation simplicity. The transmitted image is the standard Lenna image. It consists of 50 x 50 pixels and 8 bits per pixel, which therefore amounts to 20,000 bits of data.

Before transmitting BFSK image signal, 4 ms Linear Frequency Modulated (LFM) ping signal is emitted to measure the channel impulse response. at each range and depth. Its start and stop frequencies are 16 and 24 kHz, respectively. The LFM ping is emitted 30 times with interval of 1 s to get a stationary average result. MIP is obtained by matched filtering the received signal with emitting ping signal. It is also used for time synchronization of the received signal for demodulation.

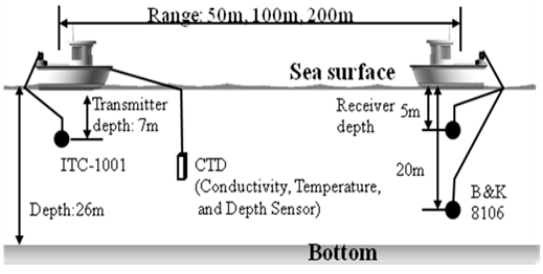

Fig. 1. Experimental configuration of underwater acoustic communication.

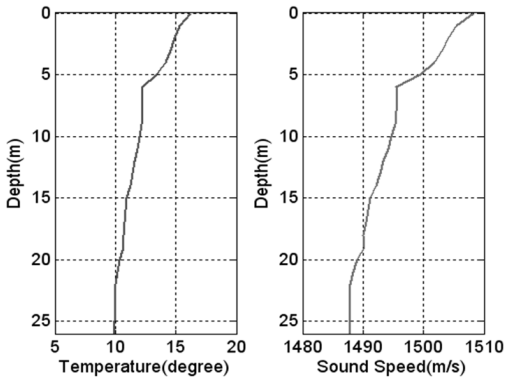

Fig. 2. Temperature and sound velocity profiles of experimental site.

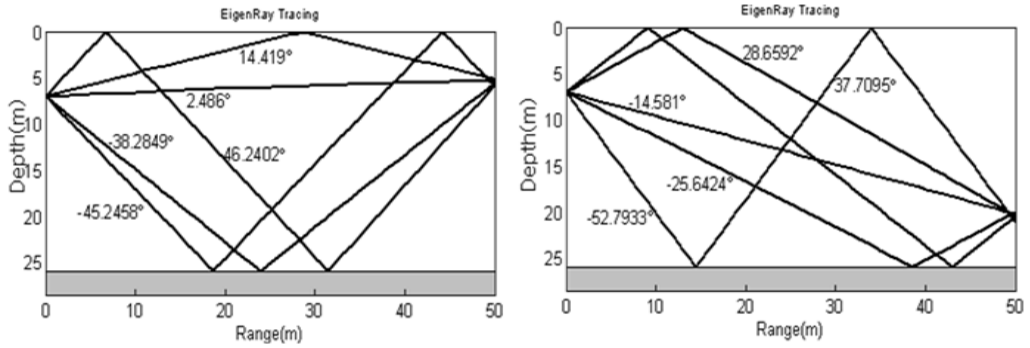

(a) 50 m Tx-Rx range eigenrays trace

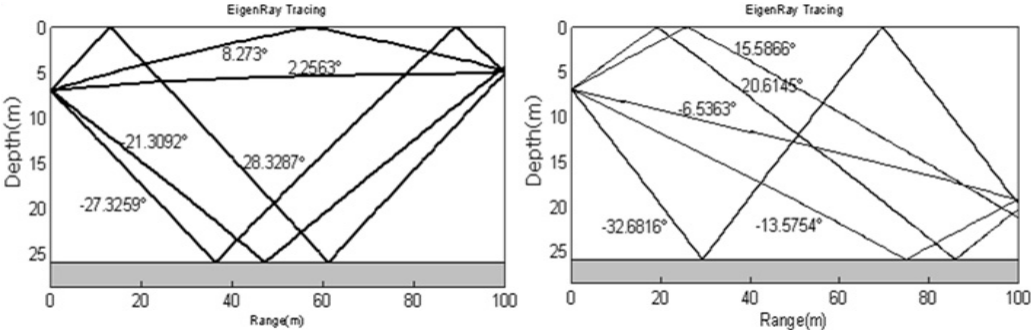

(b) 100 m Tx-Rx range eigenrays trace

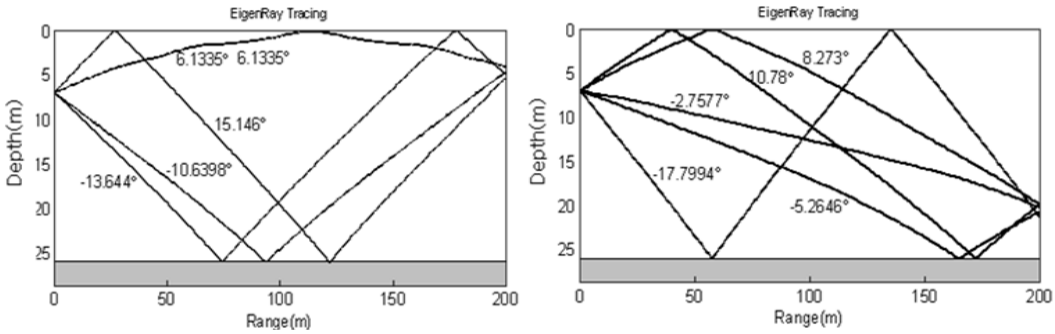

(c) 200 m Tx-Rx range eigenrays trace

Fig. 3. Simulated eigenray trace results of two different receiver depths and three different Tx-Rx ranges: receiver depth 5 m (left) and 20 m (right).

IV. Results and Discussion

Fig. 2 and Fig. 3 show the sound velocity profile and the eigenray trace results, respectively. In Fig. 3, the numerical value of each eigenray means grazing angle with respect to boundary plane. The angle of direct path ray is measured to horizontal direction. Only the first five arrivals which could show high signal amplitude, are shown in Fig. 3.

The measured MIPs for corresponding receiver depths and transmitter-receiver ranges are shown in Fig. 4. In the measured MIP's, the simulated 5 eigenrays are not clearly shown except the direct path due to scattering and energy loss in boundaries. Surface wave height and a critical angle of bottom are about 0.7 m and 15^{o}[6], respectively.

At 5 and 20 m receiver depths in 50 m Tx-Rx range, only the direct and the surface reflected path signals are shown. This explains that grazing angles of bottom path signals are greater than the critical angle and highly

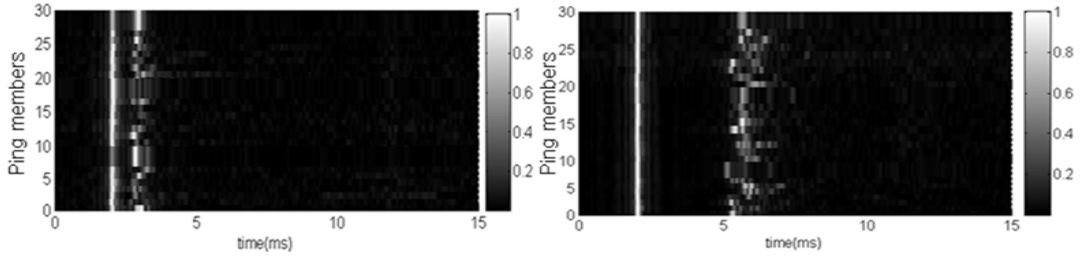

(a) 50 m Tx-Rx range

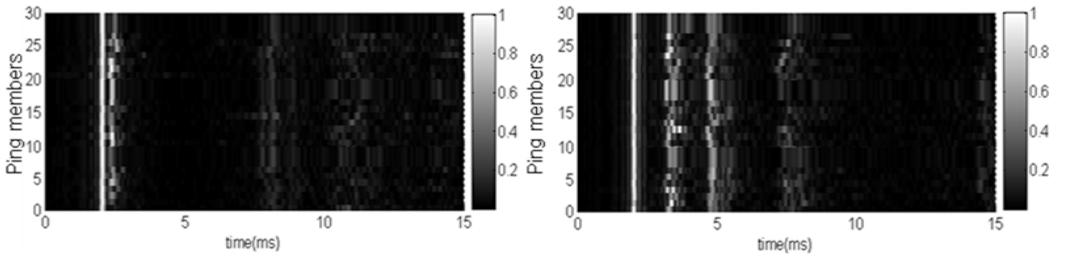

(b) 100 m Tx-Rx range

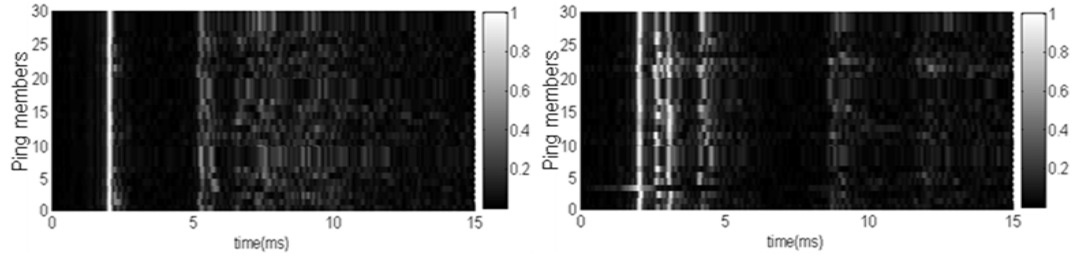

(c) 200 m Tx-Rx range

Fig. 4. Measured impulse responses for two different receiver depths and three different Tx-Rx ranges: receiver depth 5 m (left) and 20 m (right).

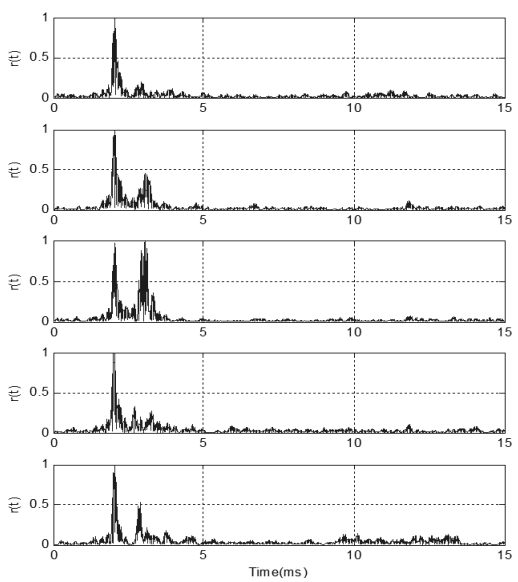

Fig. 5. Five MIPs samples at 5 m receiver depth in Tx-Rx range 50 m.

Table 1. RMS delay spread τ_{rms} and channel coherence bandwidth B_c of three different TX-Rx ranges and two different receiver depths.

Tx-Rx range/receiver depth	τ_{rms} (ms)	B_c (Hz)
50 m / 5 m	0.23	590
50 m / 20 m	1.08	180
100 m / 5 m	0.18	1100
100 m / 20 m	0.62	320
200 m / 5 m	0.11	1820
200 m / 20 m	0.34	600

attenuated in sandy mud bottom.

In 100 m Tx-Rx range, only direct and surface reflected path signals are shown. at 5 m receiver depth but the bottom reflected signals are also shown at 20 m receiver depth since grazing angles of bottom reflected path signals are less than or not much greater than the critical angle.

Fig. 6. Images of Tx-Rx range 50 m at 5 m receiver depth: (a) 100, (b) 200, (c) 500, and (d) 1000 bps.

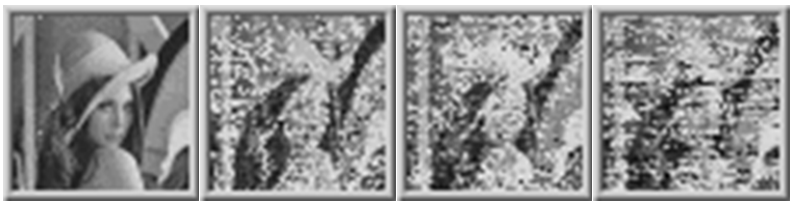

Fig. 7. Images of Tx-Rx range 50 m at 20 m receiver depth: (a) 100, (b) 200, (c) 500, and (d) 1000 bps.

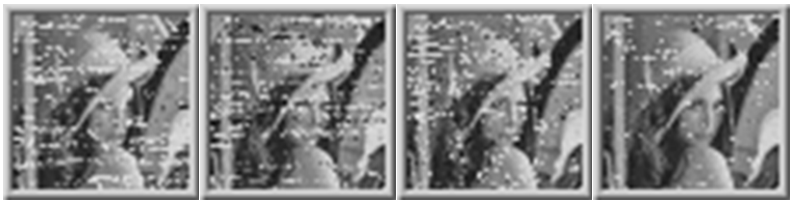

Fig. 8. Images of Tx-Rx range 100 m at 5 m receiver depth: (a) 100, (b) 200, (c) 500, and (d) 1000 bps.

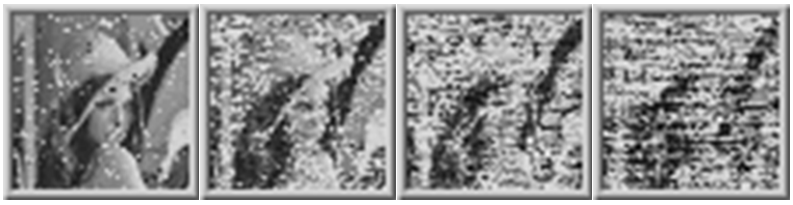

Fig. 9. Images of Tx-Rx range 100 m at 20 m receiver depth: (a) 100, (b) 200, (c) 500, and (d) 1000 bps.

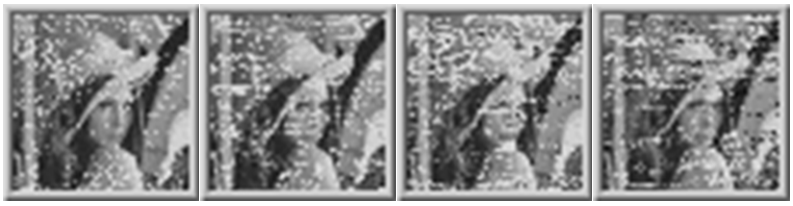

Fig. 10. Images of Tx-Rx range 200 m at 5 m receiver depth: (a) 100, (b) 200, (c) 500, and (d) 1000 bps.

Fig. 11. Images ofTx-Rx range 200 m at 20 m receiver depth: (a) 100, (b) 200, (c) 500, and (d) 1000 bps.

In 200 m Tx-Rx range, all the grazing angles of bottom reflected path signals are less than or not much greater than the critical angle. Therefore, all the 5 eigenray path signals are shown at 20 m depth but not at 5 m depth due to highly scattering in the sea surface. The direct and the first arrival surface reflected eigenrays are congested together and other surface reflected signals are highly scattered due to high grazing angle to rough sea surface.

The MIPs in Fig. 4 are evaluated using eqn. (4)-(6). Figure 5 shows five MIPs samples at 5 m receiver depth in Tx-Rx range 50 m. The 30 pings' MIPs are averaged and dominant paths are selected by -6 dB threshold to ignore the low level scattered signal. Table 1 shows RMS delay spread τ_{rms} and channel coherence bandwidth B_c of two different receiver depths and three different Tx-Rx ranges.

As shown in Tab. 1, B_c is dependent on both Tx-Rx range and receiver depth. At the deeper receiver, B_c is the narrower due to high absorption at bottom and more scattering at sea surface.

Figures 6-11 are the received images for three different Tx-Rx ranges and two different receiver depths. To change the channel's frequency selectivity for given B_c, four different transmission bit rates such as 100, 200, 500, and 1000 bps are used. The signal bandwidths B_s are equal to 100, 200, 500, 1000 Hz since BFSK is adopted in modem.

In Fig. 6 for 5 m depth receiver, the images of 100, 200, and 500 bps are better than that of 1000 bps. The B_s of 1000 bps is greater than B_c as shown in Tab. 1. In Fig. 7, however, only the image of 100 bps is better than other since the B_s of other three are greater than B_c of 180 Hz in this channel.

In Fig. 8 for 5 m depth receiver, all the images of 100, 200, 500 and 1000 bps have similar quality. Since the B_c in this channel is 1100, each B_s are less than B_c of 1100 in the channel. In Fig. 9, however, the image of 100 bps is the best since B_c in this channel. is 320 Hz.

In Fig. 10 and 11 for 5 and 20 m depth receiver, all the images have a similar quality. The B_c of the former is 1820 Hz and that of the latter is 600 Hz.

Table 2. BER of transmission rate at each transmitter-receiver range and each receiver depth.

range (m)	depth (m)	100 bps	200 bps	500 bps	1000 bps
50	5	0.014	0.008	0.025	0.198
	20	0.001	0.163	0.198	0.212
100	5	0.066	0.024	0.080	0.085
	20	0.030	0.147	0.289	0.085
200	5	0.057	0.084	0.110	0.099
	20	0.082	0.047	0.091	0.119

In Figs. 8-11, each image quality is also highly affected by background noise by long Tx-Rx range.

Considering Tx-Rx range with respect to image quality, images at shorter range are more dependent on receiver depth. The quality of images in 200 m range is less dependent on the receiver depth. This could be explained by the fact that the effective delay spreads of both receiver depths are similar to each other since grazing angle of each dominant eigenray to bottom and sea surface are similar to each other due to long Tx-Rx range. This is confirmed in Tab. 1 in which B_c of 200 m range is smaller than those of 50 and 100 m range.

The BER of transmission rate of each experimental condition is summarized in Tables 1 and 2.

V. Conclusions

Underwater image transmission performance of BFSK is examined in very shallow littoral zone and analyzed to evaluate the grazing-angle dependent boundary reflection effects on underwater acoustic communication.

The received image quality is highly dependent on the transmitter-receiver range and receiver depth which characterize the channel coherence bandwidth.

The higher grazing-angle reflection eigenrays induce high absorption at bottom and severe scattering at rough sea surface. This gives the better image quality. The lower grazing-angle eigenrays at the longer transmitter-receiver range gives the higher signal amplitude and the image quality is not degraded since they are congested to give shorter delay spread. Image quality or BER in shorter range is more receiver depth dependent than that in longer range.

Acknowledgement

This work was supported by Research Programs of Hanwha Corporation 2011.

References

1. J. Han, K. Kim, Y. Yoon, H. Mun, S. Chun, and K. Son, "Sea trial results of the direct sequence spread spectrum underwater acoustic communication in the East Sea" (in Korean), J. Acoust. Soc. Kr, **31**, 441-448 (2012).
2. H. Kim, D. Choi, J. Seo, J. Chung, and S. Kim, "The experimental verification of adaptive equalizers with phase estimator in the east sea" (in Korean), J. Acoust. Soc. Kr, **29**, 229-236 (2010).
3. H. Kim, J. Seo, J. Kim, S. Kim, and J. Chung, "Equalizer mode selection method for improving bit error performance of underwater acoustic communication systems" (in Korean), J. Acoust. Soc. Kr, **31**, 1-10 (2012).
4. H. Ko, S. Lee, M. Kim, D. Cho, K. Kim, B. Park, J. Park, and Y. Lim, "Performance analysis of spatial correlation for underwater channel environments" (in Korean), J. Acoust. Soc. Kr, **31**, 107-113 (2012).
5. W. B. Yang, and T. C. Yang, "High-frequency channel characterization for M-ary frequency-shift-keying underwater acoustic communications," J. Acoust. Soc. Am. **120**, 2615-2626 (2006).
6. M. Siderius, M. Poter, P. Hursky, V. McDonald, and the KauaiEx Group, "Effects of ocean thermocline variability on noncoherent underwater acoustic communications," J. Acoust. Soc. Am. **121**, 1895-1908 (2007).
7. Y. Isukapalli, H. C. Song, and W. S. Hodgikiss, "Stochastic channel simulator based on local scattering functions," J. Acoust. Soc. Am., **130**, EL200-205 (2011).
8. J. Park, K. Park, and J. R. Yoon, "Underwater acoustic communication channel simulator for flat fading," Jpn. J. Appl. Phys., **49**, 07HG10 (2010).
9. R. J. Urick, *Principles of Underwater Sound*, 3rd ed., (McGraw-Hill, NewYork, 2001).
10. B. Borowski, "Characterization of a very shallow water acoustic communication channel," B. Borowski, "Characterization of a very shallow water acoustic communication channel," in proceedings of MTS/IEEE OCEANS'09 Conference (IEEE, Biloxi),1-10 (2009).
11. J. Kim, K. Park, J. Park, and J. R. Yoon, "Coherence bandwidth effects on underwater image transmission in multipath channel," Jpn. J. Appl. Phys., **50**, 07HG05 (2011).
12. J. G. Proakis, *Digital Communications*, 4th ed. (McGraw-Hill, NewYork, 2001).

저자 약력

▸ Kyu-Chil Park

He received the B.S. and M.S. degrees in Department of Electronic Engineering from Pukyong National University, Busan, Korea in 1993 and 1995, respectively and the Ph.D. degree in Division of Science and Technology for Intelligence, Graduate School of Natural Science and Technology from Okayama University, Okayama, Japan in 2000. Since 2002, he has been a Professor in Department of Information and Communications Engineering, Pukyong National University, Busan, Korea. His research interests include Underwater Acoustic Signal Processing, Adaptive Signal Processing, Numerical Analysis, Optimization and Inverse Problem in Engineering.

▸ Jihyun Park

He received the B.S. degree in Telematics engineering from Busan National University in 2000, and the M.S. and Ph.D. degrees in telematics engineering from Pukyong National University in 2002 and 2008, respectively. His current research interests include digital signal processing and underwater acoustic communication system design

▸ Seung Wook Lee

He received the B.S. degree in Elecrtonics Engineering from Kyungpook National University in 1989. Since 1989, he has been a chief research engineer, Development Team 2, Gumi plant, Hanwha Corporation. His current research interests include underwater signal processing.

▸ Jin Woo Jung

He received the B.S. and M.S. degrees in Information and Communication Engineering from Soongsil University in 2007 and 2009. His current research interests include underwater signal processing.

▸ Jungchae Shin

He received the B.S. degree in Elecrtonics and Elecrtical Engineering from Kyungpook National University in 2002, and the M.S. degrees in Information and Communication from Kyungpook National University 2004, and Ph.D. degrees in Elecrtonics Engineering from Kyungpook National University 2010. Since 2010, he has been a Senior Research Engineer, Development Team 2, Gumi plant, Hanwha Corporation. His current research interests include underwater signal processing, and network

▸ Jong Rak Yoon

He received the M.S. and Ph.D degrees in ocean engineering from Florida Atlantic University in 1987 and 1990, respectively. From 1979 to 1985, he had worked at Agency for Defense Development as a research scientist. Since 1990, he has been a faculty member in Department of Information and Communication Engineering, Pukyong National University. His primary interests are underwater acoustics and acoustic signal processing, with emphasis on underwater acoustic signal measurement, analysis, classification and underwater acoustic communication.